



**OPEN**  
**DATA DESCRIPTOR**

# Electricity use in big area additive manufacturing of fiber-reinforced polymer composites

Hao Chen<sup>1</sup>✉, Srikanth Pilla<sup>2,3,4,5</sup>, Gang Li<sup>6</sup>, Muzan Williams Ijeoma<sup>1</sup> & Michael Carbajales-Dale<sup>1</sup>

In recent years, additive manufacturing (AM), especially large-format additive manufacturing (LFAM), has gained momentum in the manufacturing industry. While LFAM offers benefits over conventional manufacturing processes, such as minimizing material waste and providing vast geometric freedom, assessing its sustainability remains challenging due to limited data, particularly on energy consumption. Most existing data pertain to small-scale or desktop AM and are not directly applicable to LFAM. In this study, we conducted real-time measurements of electricity usage for a type of LFAM known as big area additive manufacturing (BAAM), which typically uses fiber-reinforced polymer pellets as feedstock. We collected electricity usage data from fifteen printing jobs over two months in an industrial production setting. These data fill the existing gap and can be reused to enhance the community's understanding of LFAM electricity usage, support further research, and promote sustainable development in advanced manufacturing technologies.

## Background & Summary

Additive manufacturing (AM), or 3D printing, stands at the vanguard of advanced manufacturing<sup>1</sup>. It leverages computer-aided design and precise control to print near-net shape final parts layer by layer, offering vast geometric freedom. This process minimizes material waste and has the potential to promote sustainable manufacturing practices. Most AM systems today are typically desktop or small-scale and primarily used for rapid prototyping<sup>2</sup>. However, the industry is increasingly interested in transitioning from prototyping to manufacturing end-user products and scaling up to produce large and fully functional items<sup>3,4</sup>. These products have applications in wide-ranging sectors, including aerospace<sup>5,6</sup>, automotive<sup>7–9</sup>, energy<sup>10–14</sup>, construction<sup>15</sup>, tooling<sup>16–18</sup> and marine<sup>19,20</sup>.

Large-format additive manufacturing (LFAM) represents a considerable advancement in AM technology. AM systems with a print volume exceeding one cubic meter can be classified as LFAM, which offers higher throughput and energy efficiency than desktop systems<sup>20–23</sup>. LFAM processes vary based on the material—such as metal, ceramic, polymer, and fiber-reinforced composites—and technologies employed, including vat photopolymerization, powder bed fusion, and material extrusion<sup>23,24</sup>. Among these technologies, Big Area Additive Manufacturing (BAAM) stands out. Developed by Cincinnati Incorporated and the U.S. Department of Energy's (DOE) Oak Ridge National Laboratory, BAAM features a print volume of more than 26 cubic meters (6 m by 2.5 m by 1.8 m)<sup>19</sup>.

BAAM demonstrates its high flexibility and throughput by using pellets as feedstock, unlike Fused Filament Fabrication (FFF) and Fused Deposition Modeling (FDM) systems, which use filaments<sup>25</sup>. These pellets are typically fiber-reinforced polymer composites, made by blending discontinuous fibers (typically, carbon fiber (CF) and glass fiber (GF); research is also being done on natural fibers, such as wood pulp and flour<sup>26</sup>) and thermoplastic polymers, such as acrylonitrile butadiene styrene (ABS), polyphenylene sulfide (PPS), polyethyleneimine (PEI), polyphenylsulfone (PPSU), polycarbonate (PC) and Polylactic acid (PLA)<sup>27</sup>. Since these pellets consist of short fibers (less than 3 mm)<sup>28,29</sup>, they provide greater flexibility, allowing them to be formed into complex

<sup>1</sup>Department of Environmental Engineering & Earth Sciences, Clemson University, Clemson, SC, 29634, USA. <sup>2</sup>Center for Composite Materials, University of Delaware, Newark, DE, 19716, USA. <sup>3</sup>Department of Mechanical Engineering, University of Delaware, Newark, DE, 19716, USA. <sup>4</sup>Department of Materials Science and Engineering, University of Delaware, Newark, DE, 19716, USA. <sup>5</sup>Department of Chemical and Biomolecular Engineering, University of Delaware, Newark, DE, 19716, USA. <sup>6</sup>Department of Mechanical Engineering, Clemson University, Clemson, SC, 29634, USA. ✉e-mail: [hchen4@clemson.edu](mailto:hchen4@clemson.edu)

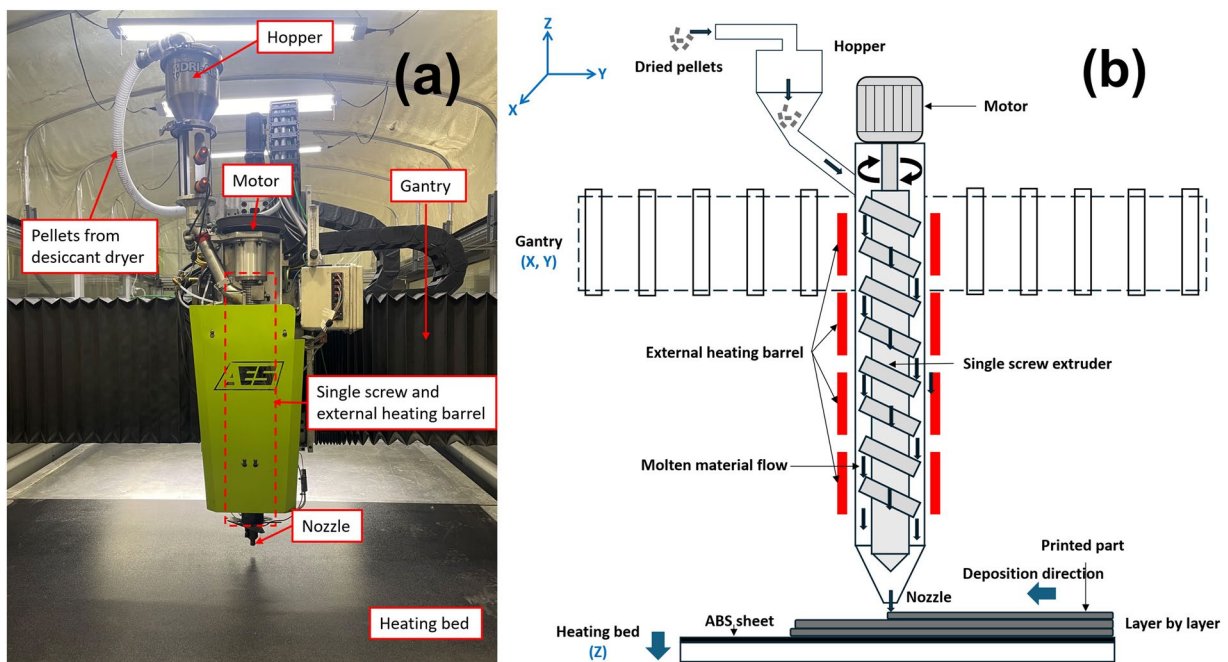


**Fig. 1** (a) Image of BAAM system. (b) Schematic of the BAAM system (adapted from<sup>16,57</sup>).

shapes. This contrasts with the continuous fiber-reinforced polymers commonly used in conventional manufacturing methods like autoclave and pultrusion. Additionally, using pellets can achieve a higher throughput, enabling the printing of large structures at process rates of up to 50 kg/h<sup>30</sup>.

As shown in Fig. 1, the BAAM system can be considered a large-scale FDM or FFF system. Before each printing job, feedstock (i.e., pellets) is placed in a desiccant dryer to remove moisture, which can affect the quality of the final product. The dried pellets are then fed into the hopper, where the rotating single screw extruder and external heating barrel generate heat to melt the pellets. The screw pushes the molten pellets, which are then extruded through the nozzle. At the same time, the gantry drive controls the x and y directions, while the heating bed controls the z direction to form the final parts. The parts are printed on a constant temperature heating bed, typically consisting of an aluminum table covered by an ABS sheet. To ensure high-quality printing, BAAM's operational parameters—such as nozzle diameter, screw speed, heating barrel temperature, gantry travel speed, pellet feeding rate, heating bed temperature, and other variables—are carefully selected and controlled based on the different feedstock materials and the geometry of the final product<sup>25,27,31</sup>.

Existing literature on energy consumption and sustainability analysis of polymer-based AM mainly focuses on desktop or small-scale systems<sup>32–45</sup>, with limited studies addressing LFAM or BAAM. Gutowski *et al.* explored the relationship between process rate and energy intensity across various manufacturing processes, demonstrating that BAAM can substantially reduce electricity consumption compared to conventional FDM technologies thanks to its higher process rate, which is comparable to mass production methods such as injection molding<sup>46</sup>. Kulkarni *et al.* performed a comparative life cycle assessment (LCA) of injection molding and BAAM to produce NdFeB-bonded permanent magnets<sup>47</sup>. Subsequently, Zhou *et al.* conducted a techno-economic assessment (TEA) using injection molding and BAAM to manufacture the same type of permanent magnet<sup>48</sup>. Notably, Kulkarni *et al.* utilized energy consumption data from a similar but smaller-scale AM process as a proxy for BAAM. Moreover, the studies by Gutowski *et al.* and Zhou *et al.* relied on data for BAAM from the U.S. Electric Power Research Institute (EPRI) in 2014. However, this data is limited to a single point and lacks material specification and operational parameters<sup>49</sup>. To the best of our knowledge, no studies have provided updated and detailed energy consumption data for LFAM since 2014, especially BAAM. To thoroughly explore the sustainability of evolving advanced manufacturing technologies, more recent and comprehensive data are essential.

To help bridge the data gap in energy requirements for LFAM, we conducted real-time measurements for a BAAM system over two months in an industrial production setting. This effort resulted in a database containing fifteen datasets of electricity use across different printing jobs. These printing jobs encompass a range of feedstock materials, including CF and GF reinforced with different polymers such as ABS, PEI, and PC, as well as parts of varying sizes and geometries.

Here, we present these datasets, which are valuable for promoting sustainable development in the field of advanced manufacturing technologies. We believe these datasets can help the community pave the way towards a better understanding of LFAM's sustainability, provide a benchmark for validating the technology, and improve the energy efficiency of the manufacturing process. Furthermore, these datasets can be used in assessment tools that support decision-making, such as LCA and TEA. In this paper, we will thoroughly describe the data collection process and analysis of the data.

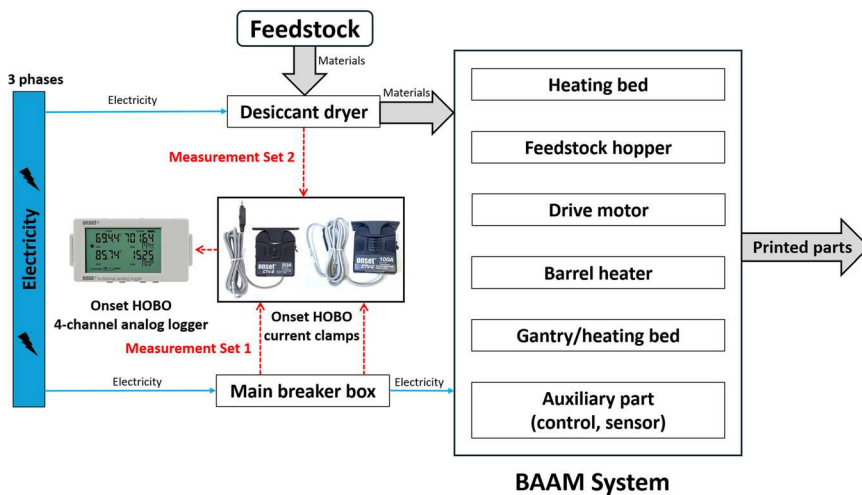


**Fig. 2** Main components of BAAM and the measurement setup.

## Methods

Our measurements were taken at Additive Engineering Solutions (AES)' manufacturing facility, located in Ohio, USA, for one of its BAAM systems. The data collection period spanned from June 2023 to August 2023.

Figure 2 shows the main components that require electricity during the operation of the BAAM system and the measurement setup. Since BAAM is an integrated system, it is challenging to measure each component individually, such as the drive motor, gantry, and external heating barrel. Therefore, we measured the electricity usage at the main cables in the main breaker box, which supply power to all components of the BAAM system. Others may use our data to study and break down energy consumption in further detail (See Usage Notes Section).

We used Onset HOBO current clamps and installed them in the main breaker box (shown as Measurement Set 1 in Fig. 2). The BAAM power supply system is an industrial three-phase voltage system and with three cables. Due to space limitations, we installed clamps on only two of the three-phase cables, using one clamp per cable. One clamp, configured as a CTV-B 50 A, has a maximum current measuring capacity of 50 A, and the other, configured as a CTV-C 100 A, has a maximum current measuring capacity of 100 A. We selected this configuration to avoid potentially exceeding the clamps' maximum measuring capacities during different print jobs (the maximum current on the nameplate of this system is 120 A). These clamps were connected to an Onset HOBO 4-channel analog logger (UX120-006M), with the measurement interval set to 10 seconds. This setup was kept in place and maintained continuously throughout the two-month measurement period without any interruptions. At the end of this period, we extracted the data from the analog logger using the HOBOware software<sup>50</sup>.

The BAAM system operates based on job requirements and was not continuously running (24/7). We only reported the electricity usage from the start to the end of each printing job, excluding periods such as machine startup, warm-up, idle time, sample printing parts, cooldown, and maintenance (See Data Record Section). The mass of each printed part was measured directly at the end of manufacturing. The voltage provided by the manufacturing facility was assumed to remain constant at 460 V throughout our measurement period. The power factor (PF) for this manufacturing facility was assumed to be 0.9.

First, the electricity usage for each print job, as measured by a single clamp, is calculated using Eq. 1. Then, the final electricity usage is determined by averaging the values obtained from both clamps.

$$E = \sum_{i=0}^n I_i \times V \times PF \times \sqrt{3} \times t \quad (1)$$

where  $I$  is the current measured for each 10-second interval;  $V$  is the voltage, which is 460 V;  $PF$  is the power factor, which is 0.9; and  $t$  is the interval, which is 10 seconds.

Moreover, specific energy consumption (SEC) is a metric, typically expressed as an average value, used in manufacturing to measure the energy consumed per unit of production output<sup>46,51,52</sup>. Here, we quantify the SEC by dividing the calculated electricity usage per printing job by the total weight of that job (Eq. 2).

$$SEC = \frac{E}{m} \quad (2)$$

where  $E$  is the final calculated electricity usage per printing job and  $m$  is the weight of that job.

The desiccant dryer is a separate system and is not part of BAAM. Beyond the BAAM measurement, we also applied the same method and measured the current of the desiccant dryer using one clamp (CTV-B 50 A), as shown as Measurement Set 2 in Fig. 2. For more information, see Data Records and Usage Notes.

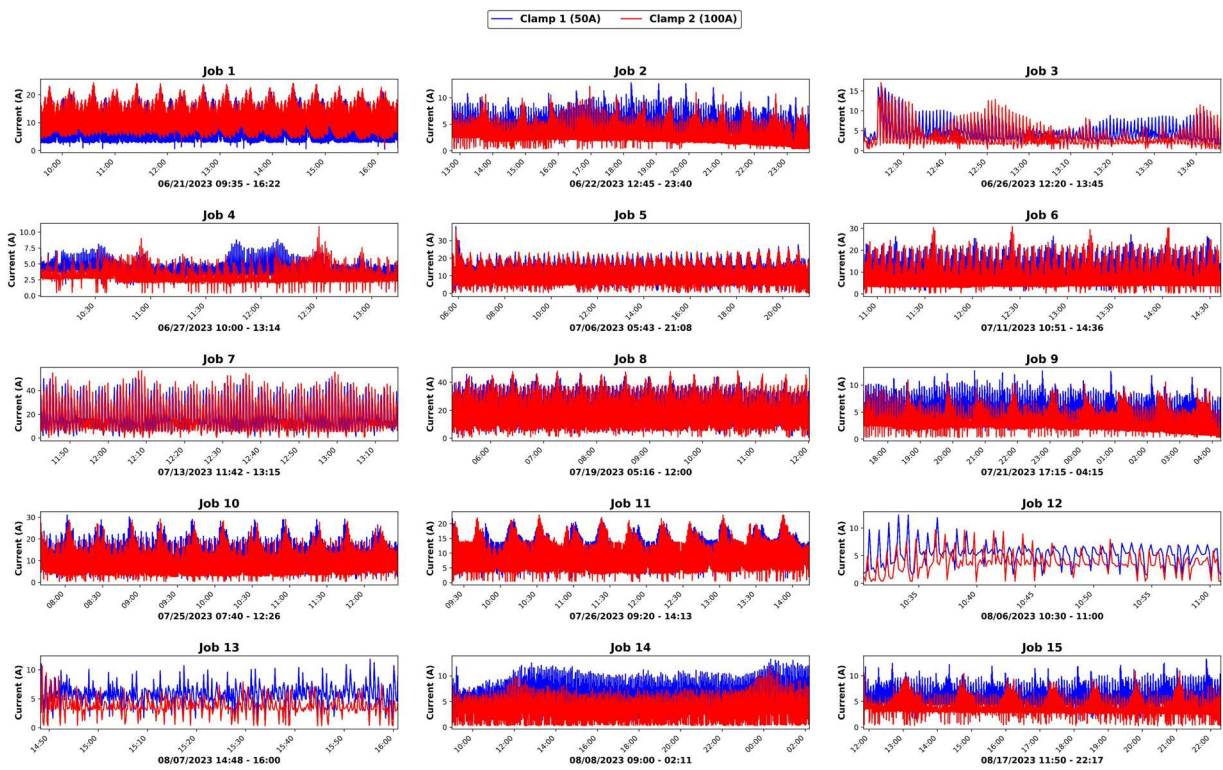


**Fig. 3** Current profiles for each printing job of the BAAM system, with the profiles for Clamp 1 (50 A) and Clamp 2 (100 A) differentiated by color.

## Data Records

The dataset is available at the Figshare repository (<https://doi.org/10.6084/m9.figshare.26311921.v2><sup>53</sup>). The file is in XLSX format and contains a total of twenty sheets.

The first sheet, “Meta Data,” includes essential information regarding each printing job (Job 1 to Job 15), such as date, start time, end time, duration, feedstock material, product weight, bed temperature, melting temperature, layer thickness, bead width, part geometry, extrusion and gantry speed. Moreover, it shows the calculated results for the processing rate, total electricity usage, and SEC for each print job based on Eqs. 1, 2.

From the second to the sixteenth sheet, labeled “Job 1” to “Job 15,” detailed current data for each printing job are recorded separately from the two clamps at 10-second intervals. The current profiles for each printing job are shown in Fig. 3.

The next sheet, labeled “Raw Data\_BAAM,” aggregates all the raw current data for both clamps. This sheet shows the continuously recorded current from the beginning of the measurement setup to the end of the measurement period. It should be noted that even outside the reported operation period for BAAM, the current value may not be zero for some periods. This may be due to machine startup, warm-up, idle periods, printing sample parts, cooling, and maintenance. However, detailed information about these periods is not included in our database.

The last three sheets provide the electricity usage data for the desiccant dryer. The ‘Desiccant Dryer Summary’ sheet includes essential information for two drying jobs: start time, end time, duration, and the drying material. It also provides statistical information on the current values, including the minimum, interquartile range, maximum, mean, and standard deviation. The ‘Desiccant Dryer-PC 20GF’ and ‘Desiccant Dryer-ABS 20CF’ sheets contain detailed current data for drying polycarbonate with 20% glass fiber (PC-20GF) and Acrylonitrile Butadiene Styrene with 20% carbon fiber (ABS-20CF) feedstock materials, respectively.

## Technical Validation

First, the measurement setup was maintained continuously throughout the two-month period without any interruptions, and we accurately recorded the start and end times of each printing job. Therefore, there is no missing data in our database.

Second, the manufacturer’s specifications indicate that the accuracy of the current clamps and analog logger is  $\pm 2.1\%$ , which falls within our acceptable range<sup>54</sup>.

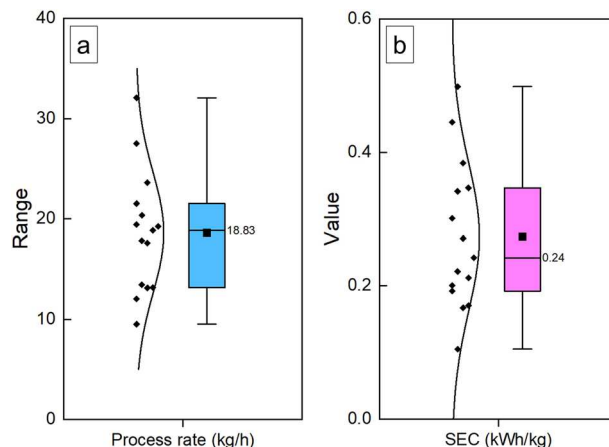
Third, the current data recorded by both clamps did not exceed the lower maximum capacity of 50 A, verifying that all obtained current data were valid except for Job 7, where the maximum current recorded was 56.72 A from the clamp with a maximum capacity of 100 A.

Fourth, Table 1 shows the statistical summary of current values for each printing job. We note that there are some variations in the values (i.e., maximum, minimum, and mean) measured by these two clamps. These variations could be attributed to the load imbalance caused by the intermittent operation of BAAM components,

Job	Clamp 1–50 A (A)						Clamp 2–100 A (A)					
	Minimum	25 <sup>th</sup> percentile	50 <sup>th</sup> percentile	Maximum	Mean	Standard deviation	Minimum	25 <sup>th</sup> percentile	50 <sup>th</sup> percentile	Maximum	Mean	Standard deviation
1	0.4746	3.5080	7.2541	21.0529	8.0295	4.7236	1.6938	7.1382	9.7566	24.3595	10.7452	4.4616
2	1.3588	3.2898	4.0414	12.8321	4.4809	1.7258	0.2884	1.8326	2.3293	12.1218	2.9516	1.7731
3	1.4603	2.9290	3.5470	16.0838	4.5908	2.5682	0.3876	1.7419	2.0493	17.0565	3.3922	2.9112
4	1.5389	3.2624	3.8625	8.8815	4.1760	1.2214	0.3799	2.1611	2.6345	10.8659	3.0312	1.4146
5	1.1070	7.4935	9.9627	37.9225	10.7956	4.3782	0.0885	5.3422	9.1081	36.0906	9.6886	5.0394
6	1.3779	4.6853	5.7153	27.0436	8.2052	5.3275	0.3174	3.4161	3.9246	30.7836	7.1841	6.1286
7	1.3802	7.3198	12.9641	49.9992	17.4515	12.8189	0.3601	5.8221	10.0160	56.7193	16.7007	14.4434
8	1.8006	9.5846	13.1327	46.5988	16.7009	9.6106	0.4456	7.8504	13.2189	48.2994	16.0990	10.5033
9	1.3596	3.6572	4.2828	12.6780	4.7704	1.7704	0.2747	1.9276	2.4606	10.9468	2.9947	1.7064
10	1.3817	5.5345	8.6389	31.0323	10.3305	5.8294	0.3403	3.6046	6.6064	29.1981	8.7523	6.1471
11	1.3939	5.5743	8.6370	21.7807	9.0933	4.0961	0.3372	3.7797	6.7598	22.9267	7.9149	4.8554
12	1.4343	4.8585	5.3956	12.3545	5.2610	2.0278	0.3037	2.9652	3.4257	9.6986	3.6294	2.0515
13	1.4519	4.8314	5.6443	11.8509	5.7660	1.8579	0.3571	3.0919	3.3661	10.6310	3.6132	1.5345
14	1.3672	4.4915	5.0008	13.2670	5.4524	1.9233	0.3037	2.7970	3.0335	11.7739	3.3337	1.5229
15	1.4183	4.5525	5.1362	13.2326	5.5571	1.6108	0.2853	2.8290	3.2098	10.9483	3.5945	1.4311

**Table 1.** Statistical summary of current values for each printing job.

Source	Process rate (kg/h)	SEC (kWh/kg)
Literature	10.2 <sup>49</sup> 22.68–29.48 <sup>25</sup> 36.28 <sup>56</sup>	BAAM: 1.2 <sup>49</sup> FDM/FFF: 11.4–78.0 <sup>46,49</sup>
Our measurement	9.5–32	0.1–0.5

**Table 2.** Reported process rates and specific energy consumption values from the literature for comparison with our measurements.**Fig. 4** (a) Process rate of BAAM and (b) Specific energy consumption of BAAM. In each panel, the right side shows the boxplot, and the left side shows the data distribution. Boxplots indicate 50% of the results, whiskers show the 10<sup>th</sup> and 90<sup>th</sup> percentile, black bars within the boxes represent medians, and squares denote the means.

which are controlled by the program. Therefore, we averaged the calculated values of electricity usage, derived from the current values obtained from both clamps, to provide a more accurate measure of overall electricity usage for each print job (see Eq. 1).

Finally, we calculated the process rate and SEC values, with their distribution shown in Fig. 4. These metrics were then compared with the ranges reported in existing literature (Table 2). Due to variations in part geometry and feedstocks for different printing jobs, the calculated process rates ranged from 9.5 to 32 kg/h, with a median of 18.83 kg/h. This range aligns with the values reported in the existing literature. Similarly, the calculated SEC values ranged from 0.1 to 0.5 kWh/kg, with a median of 0.24 kWh/kg. Notably, all our SEC values are lower than those of desktop or small-scale FDM/FFF systems and are also less than the only reported value for BAAM in the existing literature, which is 1.2 kWh/kg from a 2014 study<sup>49</sup>. In the 2014 BAAM study, the measurement

system boundary was not clearly defined, and the data was outdated. Our lower SEC values may be attributed to technological advancements since then, such as increased system energy efficiency.

Through the above analyses and validation procedures, we confirmed that our datasets were reliable and accurate.

### Usage Notes

The geometry of the parts, selected feedstock material, and operational parameters, such as nozzle size, screw speed, and temperature setting, can substantially affect the electricity use of the BAAM system. Our datasets could serve as a cornerstone for further BAAM energy consumption analysis. Researchers may utilize our data to break down energy consumption by components in greater detail, such as through Fourier analysis. This can enhance our understanding of BAAM subcomponents, pinpoint energy consumption hotspots, and improve overall energy efficiency.

Similar to the study conducted by Gutowski<sup>46</sup>, these datasets can be used to derive empirical models that explore the relationship between energy intensity and process rate across different feedstocks. Such models enable comparisons between the BAAM system and other manufacturing processes, helping practitioners identify the most appropriate manufacturing approach for specific needs. Furthermore, assessment tools that support decision-making, such as LCA and TEA, are heavily reliant on data. Our study fills the existing data gap in energy requirements for LFAM. Practitioners can use our database to verify the economic feasibility of BAAM and compare its environmental impact with conventional manufacturing methods for the same product.

It is important to note that the data collected for BAAM in this study was not obtained from a controlled experimental setup. Instead, it reflects the actual electricity usage in industrial production, determined by customer-specific requirements and encompassing varying geometries. The measurements for 15 print jobs represent a typical range of customer orders in real-world scenarios. Data users can refer to the geometry figures provided in the data repository to better understand the range of geometries and make informed decisions accordingly.

One limitation of this study is that we were not able to collect data for printing the same shape while systematically varying operating parameters, such as printing trajectories, gantry travel speed, extrusion parameters (e.g., screw speed, temperature), number of layers, layer thickness, and nozzle size. Addressing this limitation in future research could provide deeper insights into how these parameters influence energy consumption. Additionally, future studies could expand the dataset to include a wider range of feedstocks and design variables (e.g., part geometries).

While we measured the electricity usage of the desiccant dryer, this data was excluded from our overall energy usage calculations for BAAM systems due to challenges in standardizing its measurements. In industry practice, feedstock materials are typically dried for several hours before each print job to minimize moisture content. At AES, the desiccant dryer runs continuously during printing jobs, with electricity usage determined as a function of printing time rather than product weight (e.g., SEC). Additionally, variations in moisture content, such as those caused by storage conditions, further complicate the standardization of measurements.

Similarly, post-processing operations, such as multi-axis CNC machining required to meet final resolution requirements, were excluded from these datasets. These operations are often necessary due to inherent limitations in the quality, resolution, and consistency of printed parts<sup>55</sup>. However, post-processing energy usage varies significantly depending on part geometry and the degree of finishing required, making it challenging to standardize within the scope of this study.

To provide a more comprehensive perspective, future research could examine the entire advanced manufacturing pathway, including processes such as feedstock material drying, LFAM, and post-process CNC machining. This approach would enable the assessment of both the energy demands of individual processes and the cumulative energy required to manufacture final parts, contributing to sustainable advanced manufacturing practices.

### Code availability

No code was developed for this work.

Received: 17 July 2024; Accepted: 4 December 2024;

Published online: 18 December 2024

### References

1. Additive Manufacturing. <https://doi.org/10.1201/9780429466236> (2019).
2. Gardan, J. Additive manufacturing technologies: State of the art and trends. *Additive Manufacturing Handbook* 149–168 <https://doi.org/10.1201/9781315119106-10> (2017).
3. Shah, J. *et al.* Large-scale 3D printers for additive manufacturing: design considerations and challenges. *International Journal of Advanced Manufacturing Technology* **104**, 3679–3693 (2019).
4. Bikas, H., Stavropoulos, P. & Chryssolouris, G. Additive manufacturing methods and modeling approaches: A critical review. *International Journal of Advanced Manufacturing Technology* **83**, 389–405 (2016).
5. Xu, W. *et al.* 3D printing for polymer/particle-based processing: A review. *Compos B Eng* **223**, 109102 (2021).
6. 3D printed tool for building aircraft achieves Guinness World Records title | ORNL. <https://www.ornl.gov/news/3d-printed-tool-building-aircraft-achieves-guinness-world-records-title>.
7. 3D Printed Shelby Cobra | Department of Energy. <https://www.energy.gov/eere/ammtm/3d-printed-shelby-cobra>.
8. Love, L. J. Utility of Big Area Additive Manufacturing (BAAM) For The Rapid Manufacture of Customized Electric Vehicles. <https://doi.org/10.2172/1209199> (2015).
9. Chesser, P. *et al.* Comparison of Polymer AM Technologies for Automotive Tooling for Composite Engines. <https://doi.org/10.2172/1761614> (2021).
10. Rallabandi, V. *et al.* Traction motor design trade-offs with additively manufactured anisotropic bonded magnets. *2023 IEEE Transportation Electrification Conference and Expo, ITEC 2023*, <https://doi.org/10.1109/ITEC55900.2023.10187005> (2023).

11. Gandha, K. *et al.* 3D printing of anisotropic Sm–Fe–N nylon bonded permanent magnets. *Engineering Reports* **3**, e12478 (2021).
12. Gandha, K. *et al.* Additive manufacturing of anisotropic hybrid NdFeB-SmFeN nylon composite bonded magnets. *J Magn Magn Mater* **467**, 8–13 (2018).
13. Gandha, K. *et al.* Additive manufacturing of highly dense anisotropic Nd–Fe–B bonded magnets. *Scr Mater* **183**, 91–95 (2020).
14. Li, L. *et al.* Big Area Additive Manufacturing of High Performance Bonded NdFeB Magnets. *Scientific Reports* **6**, 1–7 (2016).
15. Paolini, A., Kollmannsberger, S. & Rank, E. Additive manufacturing in construction: A review on processes, applications, and digital planning methods. *Addit Manuf* **30**, 100894 (2019).
16. Billah, K. M. M. *et al.* Large-scale additive manufacturing of self-heating molds. *Addit Manuf* **47**, 102282 (2021).
17. Post, B. K. *et al.* Big Area Additive Manufacturing Application in Wind Turbine Molds. <https://doi.org/10.26153/TSW/16964> (2017).
18. Kumar, V. *et al.* Hybrid manufacturing technique using large-scale additive manufacturing and compression molding for high performance composites. (CAMX Conference) I OSTI. GOV. <https://www.osti.gov/biblio/1671415> (2020).
19. Post, B. K. *et al.* Using Big Area Additive Manufacturing to directly manufacture a boat hull mould. *Virtual Phys Prototyp* **14**, 123–129 (2019).
20. Vicente, C. M. S., Sardinha, M., Reis, L., Ribeiro, A. & Leite, M. Large-format additive manufacturing of polymer extrusion-based deposition systems: review and applications. *Progress in Additive Manufacturing* **8**, 1257–1280 (2023).
21. Moreno Nieto, D., Casal López, V. & Molina, S. I. Large-format polymeric pellet-based additive manufacturing for the naval industry. *Addit Manuf* **23**, 79–85 (2018).
22. Moreno Nieto, D. & Molina, S. I. Large-format fused deposition additive manufacturing: a review. *Rapid Prototyp J* **26**, 793–799 (2020).
23. Pignatelli, F. & Percoco, G. An application- and market-oriented review on large format additive manufacturing, focusing on polymer pellet-based 3D printing. *Progress in Additive Manufacturing* **7**, 1363–1377 (2022).
24. Goh, G. D., Wong, K. K., Tan, N., Seet, H. L. & Nai, M. L. S. Large-format additive manufacturing of polymers: a review of fabrication processes, materials, and design. *Virtual Phys Prototyp* **19** (2024).
25. Roschli, A. *et al.* Designing for Big Area Additive Manufacturing. *Addit Manuf* **25**, 275–285 (2019).
26. Copenhaver, K., Lamm, M. & Hubbard, A. Development of highly filled bio-based composites for sustainable, low-cost feedstock: processing effects on porosity and fiber alignment.
27. Copenhaver, K. *et al.* Recyclability of additively manufactured bio-based composites. *Compos B Eng* **255**, 110617 (2023).
28. Ajinjeru, C. *et al.* Rheological survey of carbon fiber-reinforced high-temperature thermoplastics for big area additive manufacturing tooling applications. *Journal of Thermoplastic Composite Materials* **34**, 1443–1461 (2021).
29. Duty, C. E. *et al.* Structure and mechanical behavior of Big Area Additive Manufacturing (BAAM) materials. *Rapid Prototyp J* **23**, 181–189 (2017).
30. Nyocz, A. *et al.* Controlling substrate temperature with infrared heating to improve mechanical properties of large-scale printed parts. *Addit Manuf* **33**, 101068 (2020).
31. Chesser, P. *et al.* Extrusion control for high quality printing on Big Area Additive Manufacturing (BAAM) systems. *Addit Manuf* **28**, 445–455 (2019).
32. Haghghi, A. & Li, L. Study of the relationship between dimensional performance and manufacturing cost in fused deposition modeling. *Rapid Prototyp J* **24**, 395–408 (2018).
33. Yoon, H. S. *et al.* A comparison of energy consumption in bulk forming, subtractive, and additive processes: Review and case study. *International Journal of Precision Engineering and Manufacturing - Green Technology* **1**, 261–279 (2014).
34. Dostatni, E., Dudkowiak, A., Rojek, I. & Mikolajewski, D. Environmental analysis of a product manufactured with the use of an additive technology-AI-based vs. traditional approaches. *Bulletin of the Polish Academy of Sciences Technical Sciences* **71**, 144478 (2023).
35. Le Gentil, T., Therriault, D. & Kerbrat, O. A comprehensive methodology to support decision-making for additive manufacturing of short carbon-fiber reinforced polyamide 12 from energy, cost and mechanical perspectives. *International Journal of Advanced Manufacturing Technology* **131**, 611–622 (2024).
36. Ma, J., Harstvedt, J. D., Dunaway, D., Bian, L. & Jaradat, R. An exploratory investigation of Additively Manufactured Product life cycle sustainability assessment. *J Clean Prod* **192**, 55–70 (2018).
37. Yosofi, M., Kerbrat, O. & Mognol, P. Additive manufacturing processes from an environmental point of view: a new methodology for combining technical, economic, and environmental predictive models. *International Journal of Advanced Manufacturing Technology* **102**, 4073–4085 (2019).
38. Kazmer, D., Peterson, A. M., Masato, D., Colon, A. R. & Krantz, J. Strategic cost and sustainability analyses of injection molding and material extrusion additive manufacturing. *Polym Eng Sci* **63**, 943–958 (2023).
39. Baumers, M., Tuck, C., Wildman, R., Ashcroft, I. & Hague, R. Energy inputs to additive manufacturing: does capacity utilization matter?
40. Enemuoh, E. U. *et al.* Energy and Eco-Impact Evaluation of Fused Deposition Modeling and Injection Molding of Polylactic Acid. *Sustainability* **2021**, Vol. 13, Page 1875 **13**, 1875 (2021).
41. Jayawardane, H., Davies, I. J., Gamage, J. R., John, M. & Biswas, W. K. Additive manufacturing of recycled plastics: a ‘techno-eco-efficiency’ assessment. *International Journal of Advanced Manufacturing Technology* **126**, 1471–1496 (2023).
42. Cañado, N. *et al.* 3D printing to enable the reuse of marine plastic waste with reduced environmental impacts. *J Ind Ecol* **26**, 2092–2107 (2022).
43. Maisano, D. A. *et al.* A structured comparison of decentralized additive manufacturing centers based on quality and sustainability. *International Journal of Advanced Manufacturing Technology* **121**, 993–1014 (2022).
44. Napolitano, F., Cozzolino, E., Papa, I., Astarita, A. & Squillace, A. Experimental integrated approach for mechanical characteristic optimization of FDM-printed PLA in an energy-saving perspective. *International Journal of Advanced Manufacturing Technology* **121**, 3551–3565 (2022).
45. Yosofi, M., Kerbrat, O. & Mognol, P. Energy and material flow modelling of additive manufacturing processes. *Virtual Phys Prototyp* **13**, 83–96 (2018).
46. Gutowski, T. *et al.* Note on the Rate and Energy Efficiency Limits for Additive Manufacturing. *J Ind Ecol* **21**, S69–S79 (2017).
47. Kulkarni, S., Zhao, F., Nlebedim, I. C., Fredette, R. & P Paranthaman, M. Comparative Life Cycle Assessment of Injection Molded and Big Area Additive Manufactured NdFeB Bonded Permanent Magnets. <https://doi.org/10.1115/1.4056489> (2023).
48. Zhou, X., Paranthaman, M. P. & Sutherland, J. W. Comparative Techno-economic Assessment of NdFeB Bonded Magnet Production: Injection Molding versus Big-Area Additive Manufacturing. *ACS Sustain Chem Eng* **11**, 13274–13281 (2023).
49. Assessing the Energy Consumption and Energy Intensity of Additive Manufacturing: Industrial Center of Excellence Application Guide. <https://www.epri.com/research/products/00000003002002243>.
50. HOBOware - Software Updates | Onset's HOBO and InTemp Data Loggers. <https://www.onsetcomp.com/support/help-center/software/hoboware>.
51. Gutowski, T., Dahmus, J. & Thiriez, A. *Electrical Energy Requirements for Manufacturing Processes*.
52. Li, W. & Kara, S. An empirical model for predicting energy consumption of manufacturing processes: a case of turning process. **225**, 1636–1646 <https://doi.org/10.1177/2041297511398541> (2011).
53. Chen, H., Srikanth, P., Li, G., Ijeoma, M. & Carbajales-Dale, M. Electricity Use in Big Area Additive Manufacturing of Fiber-Reinforced Polymer Composites. *figshare* <https://doi.org/10.6084/m9.figshare.26311921.v2> (2024).

54. CTV-x | Onset's HOBO and InTemp Data Loggers. <https://www.onsetcomp.com/products/sensors/ctv-x#specifications>.
55. Najmon, J. C., Raeisi, S. & Tovar, A. Review of additive manufacturing technologies and applications in the aerospace industry. *Additive Manufacturing for the Aerospace Industry* 7–31 <https://doi.org/10.1016/B978-0-12-814062-8.00002-9> (2019).
56. Jackson, R. *et al.* Overview of the Oak Ridge National Laboratory Advanced Manufacturing Integrated Energy Demonstration Project: Case Study of Additive Manufacturing as a Tool to Enable Rapid Innovation in Integrated Energy Systems. <https://doi.org/10.1115/IMECE2016-66256> (2017).
57. Pappas, J. M., Thakur, A. R., Leu, M. C. & Dong, X. A comparative study of pellet-based extrusion deposition of short, long, and continuous carbon fiber-reinforced polymer composites for large-scale additive manufacturing. *Journal of Manufacturing Science and Engineering, Transactions of the ASME* 143 (2021).

## Acknowledgements

This work was supported as part of the Artificially Intelligent Manufacturing Paradigm for Composites (AIM for Composites), an Energy Frontier Research Center (EFRC) funded by the U.S. Department of Energy, Office of Science, Basic Energy Sciences (BES) at Clemson University under Award DE-SC0023389. H.C and M.C.-D acknowledge partial publication fee support provided through Clemson University Libraries Open Access Publishing Fund. Additionally, the authors would like to acknowledge our collaborators at Additive Engineering Solutions, LLC, Ohio, USA, for their support during the measurement process and for providing 3D process-related information.

## Author contributions

H.C. conceptualized the research, collected data, conducted analysis, and drafted the manuscript under the guidance of M.C.-D. S.P., G.L. and M.W.I. reviewed the manuscript. M.C.-D. supervised the overall research, reviewed, and edited the manuscript.

## Competing interests

The authors declare no competing interests.

## Additional information

**Correspondence** and requests for materials should be addressed to H.C.

**Reprints and permissions information** is available at [www.nature.com/reprints](http://www.nature.com/reprints).

**Publisher's note** Springer Nature remains neutral with regard to jurisdictional claims in published maps and institutional affiliations.

 **Open Access** This article is licensed under a Creative Commons Attribution-NonCommercial-NoDerivatives 4.0 International License, which permits any non-commercial use, sharing, distribution and reproduction in any medium or format, as long as you give appropriate credit to the original author(s) and the source, provide a link to the Creative Commons licence, and indicate if you modified the licensed material. You do not have permission under this licence to share adapted material derived from this article or parts of it. The images or other third party material in this article are included in the article's Creative Commons licence, unless indicated otherwise in a credit line to the material. If material is not included in the article's Creative Commons licence and your intended use is not permitted by statutory regulation or exceeds the permitted use, you will need to obtain permission directly from the copyright holder. To view a copy of this licence, visit <http://creativecommons.org/licenses/by-nc-nd/4.0/>.

© The Author(s) 2024